2019 Latin American Robotics Symposium (LARS), 2019 Brazilian Symposium on Robotics (SBR) and 2019 Workshop on Robotics in Education (WRE)

Rigorous Tracking of Weld Beads for the Autonomous Inspection with a Climbing Robot

Vinicius de Vargas Terres[1], Andre Schneider de Oliveira[2], Higor Barbosa Santos[3], Lucia Valeria Ramos de Arruda[4], Flavio Neves-Jr[5], Joao Alberto Fabro[6] and Julio Endress Ramos[7]

***Abstract*— This article presents a novel strategy for an autonomous inspection robot for oil industry tanks. The goal is to identify and track the external weld beads of a tank by an inspection robot. The chosen robot is an autonomous climbing robot with differential magnetic wheels. The detection of the weld bead is made with a line profile sensor. An algorithm is proposed to identify the weld bead position from the robot. The control is designed with the Fuzzy technique. The approach is evaluated on a real plate and a cylindrical tank virtually designed with the same characteristics that real tank projects.**

I. INTRODUCTION

The storage of oil and its by-products is an activity that requires a level of caution because of the high risk of material, environmental, and physical damage. Tank inspections are tasks that require a considerable amount of time, because of reduced access and insalubrity of the place. The application of mobile robotics in this industry is aimed at creating a product that mitigates the time demanded and, consequently, operational costs.

The storage tanks require frequent inspections to avoid or minimize the risk of failures and leaks. The inspection is traditionally realized through the Non-Destructive Testing (NDT) techniques, like ultrasound. Its study object is the structural failures in the weld beads. Nonetheless, the robot needs to identify and navigate along the weld bead to be capable of inspecting the storage tanks.

Due to the size of the weld bead, its recognition is not a simple task. The [1] showed a technique for reliable weld line detection. A laser projection is appied in the weld line. The reflection of the laser is captured by a CCD camera. Based on the images collected, the weld line location is defined utilizing the Hidden Markov Model.

A similar approach is used in [2] for implementing a weld bead tracking control. The author applied the same method of the previous work to detect the weld bead. However, data processing is different. The method of least-squares regression is proposed to estimate the weld bead by a continuous curve.

[3] presented a mobile robot, which can grind automatically the welding-bead remained in the job of shipbuilding. The identification of the weld track is made with a vision-based method in these two works.

In these three articles, it is possible to observe that the vision-based method is highly influenced by the ambient light condition. Other disadvantages, when compared to laser sensors, are the measurement accuracy and the effort of processing the information received.

These differences are seen in [4] and [5]. The first author proposed a detection based on a Laser Displacement Sensor (LDS) for the weld seam. The second author selected a laser scanner for recognizing the position of the weld bead.

The control methods vary according to the robot selected and its application. [2] utilized a nonlinear controller to set the desired velocities. The reason for the choice is the nonlinear nature of the robot kinematics. [6] chose an approach based on the PID controllers to position and posture the mobile robot.

[4] proposed a Sliding Mode Controller (SMC) with a low-pass filter for controlling the robot's velocity. It is grounded in the theories of sliding mode for robust control for compensating disturbances. [5] designed a PID controller for the angular and the linear velocity of the robot. The estimation of the angle is implemented with an Extended Kalman Filter, once the laser scanner did not measure the angle of the robot.

All the approaches chosen in the works analyzed assumed a deep knowledge in the robot's kinematics. With a Fuzzy approach, a more simple design is possible. Furthermore, the integration of multiple inputs and outputs variables raises the complexity of the systems. In this case, the Fuzzy is an excellent option to model the controller, as shown in [7], [8].

The goal of this article is to identify and track the external weld beads of a tank by an inspection robot. The inspection climbing robot used is the Autonomous Inspection Robot version 1 (AIR-1) [9], [10], [11]. The line profile sensor LRS36/6 is its perception source selected. An algorithm is proposed to identify the weld bead position about the robot. A Fuzzy controller is designed for controlling the trajectory of the robot.

The paper is organized as follows. Section II presents the Autonomous Inspection Robot and its perception source. Section III describes the filter applied in the signal. Section IV describes the method utilized to find the weld bead.

*This project was partially funded by National Counsel of Technological and Scientific Development of Brazil (CNPq), Coordination for the Improvement of Higher Level People (CAPES) and Petrobras.

[1], [2], [3], [4], [5] and [6] are with Universidade Tecnológica Federal do Paraná (UTFPR), Av. Sete de Setembro, 3165, Curitiba, Paraná, Brazil

[1]Terres, V. de V. viniciusterres@alunos.utfpr.edu.br

[2]de Oliveira, A. S. andreoliveira@utfpr.edu.br

[3]Santos, H. B. higorsantos@alunos.utfpr.edu.br

[4]Arruda, L. V. R. de lvrarruda@utfpr.edu.br

[5]Neves-Jr, F. neves@utfpr.edu.br

[6]Fabro, J. A. fabro@utfpr.edu.br

[7]Ramos, J. E., CENPES, Rio de Janeiro RJ, 21941-915, Brazil julio.ramos@petrobras.com.br

978-1-7281-4268-5/19/$31.00 ©2019 IEEE
DOI 10.1109/LARS-SBR-WRE48964.2019.00051

Section V shows the design of the robot controller. Section VI analyses the experimental results of the approach. Section VII concludes the article and shows future works.

II. AUTONOMOUS INSPECTION ROBOT

The Autonomous Inspection Robot version 1 (AIR-1) was designed to navigate and inspect large metallic surfaces, like liquefied petroleum gas (LPG) storage tank. The mechanical structure of the robot is displayed in Figure 1. It is composed of two parallel groups of magnetic wheels. Each group is connected by a v-belt and is controlled by a motor. The AIR-1 has two degrees of freedom and works as a differential wheeled robot. More data about the robot can be found in [10].

Fig. 1: Autonomous Inspection Robot 1.

The robot has two primary sources in the perception system. The profile sensor is used to locate the weld beads. The model selected for this work is the LRS36/6, shown in Figure 2. It can read 376 points along 40 degrees with a distance resolution of 1 millimeter. More information about the sensor can be found in [12]. An accelerometer is used to measure the influence of gravity on the robot.

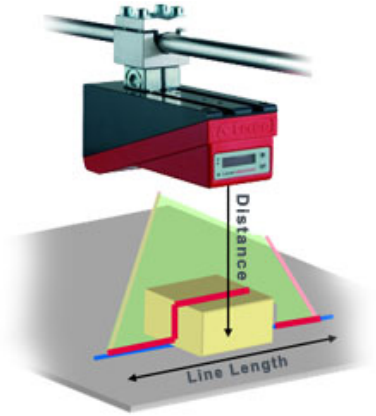

Fig. 2: Line Profile Sensor [12].

III. DATA FILTERING

A digital low-pass filter is proposed for reducing the noise in the signal received. The filter implemented is a FIR with a Kaiser window. The Equation 1 shows the window expression proposed by Kaiser, where α is $M/2$, $I_0()$ is the zeroth-order modified Bessel function of the first kind and β and M are parameters of the window [13].

$$w[n] = \begin{cases} \frac{I_0[\beta\sqrt{1-[(n-\alpha)/\alpha]^2}]}{I_0(\beta)}, & 0 \leq n \leq M \\ 0, & otherwise \end{cases} \quad (1)$$

The Equations 2 and 3 display the applied formulas to get the filter parameters. β is the Kaiser window parameter. A is the ripple height in dB. M is the order of the filter. $\Delta\omega$ is the transition bandwidth [13].

$$\beta = \begin{cases} 0, & A < 21 \\ 0.5842(A-21)^{0.4} + 0.07886(A-21), & 21 \leq A \leq 50 \\ 0.1102(A-8.7), & A > 50 \end{cases} \quad (2)$$

$$M = \frac{A-8}{2.285\Delta\omega} \quad (3)$$

The chosen values for the parameters A and $\Delta\omega$ are 80 dB and 0.05, respectively. The cutoff frequency is 0.2. Figure 3 shows the frequency response of the filter.

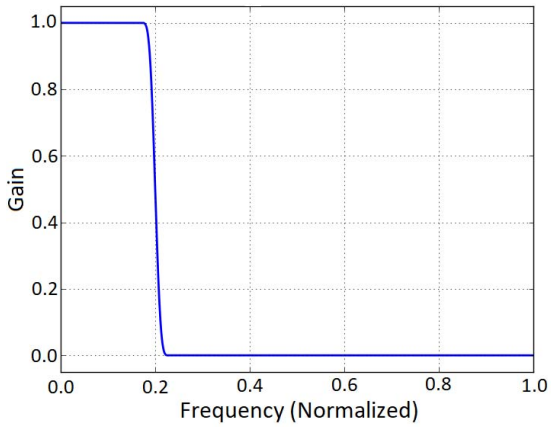

Fig. 3: Frequency response of the filter.

IV. WELD BEAD RECOGNITION

Algorithm 1 is designed to find the weld bead and its distance from the robot. The input of the system is the distance vector measured by the line profile sensor. The outputs are the distance between the center of the weld bead and the center of the robot, which is called alignment error, and the robot orientation error.

Initially, the weld bead limits must be determined. The input data is differentiated with respect to the x-axis. Then, the location of the maximum and minimum values of the derivative function is calculated. To determine if these values are the weld bead border, they are compared with a threshold

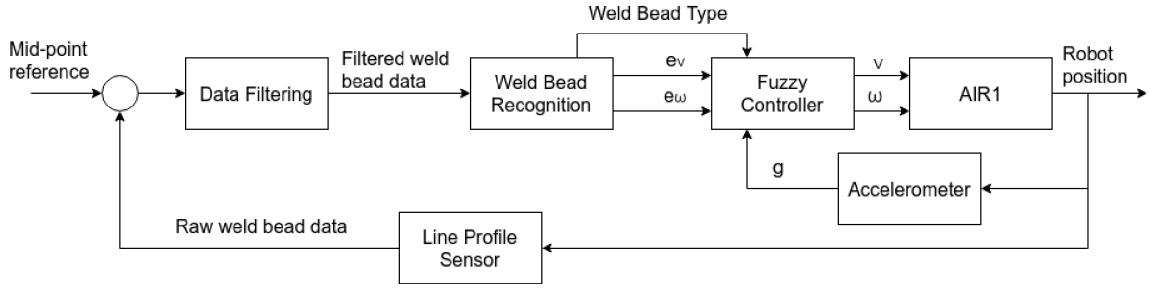

Fig. 4: Block diagram of control loop.

value. If there are not two borders, it means that the robot is on a weld bead joint. In this case, the orientation error and the weld bead joint type is set. If there are two borders in the data, the data measured is linearized.

The reason for this procedure is the reduction of the influence of tank curvature. The tank estimation algorithm is applied to linearize the signal. The linearized signal is obtained subtracting the tank position from the filtered signal. The next step is the calculation of the center of the weld bead, which is the mean value of the weld bead limits. Finally, the output data is calculated and transmitted to the controller.

Algorithm 1: Weld bead recognition

Input: Vector with the filtered data from the line profile sensor
Output: Alignment error
Output: Orientation error

```
Calculate the derivative of the input data;
Find the maximum and the minimum value of the derivative;
Evaluate if these values are considered borders;
if Data with 2 borders then
    Apply the tank estimation algorithm;
    Generate linearized signal;
    Calculate the weld bead center position;
    Calculate the alignment error of the robot;
else
    Identify the kind of the joint;
    Set the orientation error value;
    Set the weld bead joint type;
return
```

Algorithm 2 is implemented to estimate the position of the tank, and the signal is separated into three parts. The first one is from the begin until the first weld bead border. The second one is in the middle of the weld bead borders. The last one is from the previous weld bead border until the end. The second part is estimated by a straight line, using the weld bead borders. After this, the three sections are unified into a single vector.

The method of least-squares is applied for estimating the tank position in the first and the last section of the weld bead profile. The second-order polynomial is proposed to suit the

Algorithm 2: The tank estimation

Input: Vector with the filtered data from the line profile sensor
Output: Vector with the tank estimation

```
Divide the signal into three parts;
Apply the least-square method in the first and the third parts;
Estimate the tank position in the second part;
Unify the three sections;
return
```

data. The information from the line profile sensor comprises the weld bead position in the x-axis and z-axis (x_i, z_i) where i=1,2,...,n and n is the length of the data used in the least-squares regression algorithm. The estimated tank position ($\widehat{x}$, $\widehat{z}$) is calculated in the Equation 4, where a_0, a_1 and a_2 are constants of the quadratic polynomial [14].

$$\begin{aligned} \widehat{x} &= x \\ \widehat{z} &= a_0 + a_1 x + a_2 x^2 \end{aligned} \tag{4}$$

V. CONTROL DESIGN

The trajectory controller is designed applying the Fuzzy control technique. It is chosen because of the reduction of the robot's kinematics influence in the design of the controller. Another reason is its ease of design and application. Figure 4 displays the block diagram of the control loop.

The controller has four inputs and two outputs. The first input is the distance between the robot alignment center and the weld bead center, which acronym is EX. In other words, it is the error in the robot alignment. Its value is received from the weld bead recognition algorithm. The linguistic variables for this input are defined as: Negative Big (EX0), Negative Small (EX1), Zero (EX2), Positive Small (EX3), and Positive Big (EX4).

The second input is the robot orientation error, which acronym is EY. It is used for turning at the weld bead joints. Its value is calculated based on the robot odometry and joint presence. When a joint is discovered, the robot randomly chooses the path. If a turn is needed, the error is added or subtracted by a $\pi/2$ value. The linguistic variables for this input are defined as: Negative Big (EY0), Negative Medium

(EY1), Negative Small (EY2), Zero (EY3), Positive Small (EY4), Positive Medium (EY5) and Positive Big (EY6).

The third input is the type of the weld bead joint, once the robot needs more velocity depending on the joint. Its acronym is TS. The linguistic variables for this are defined as Two Turn Joint(TS0), One Turn Joint (TS12) and No Joint(TS3). The fourth input is gravity. This input is applied to identify when the robot goes up or down. Its acronym is GX. The accelerometer gives this information to the controller. The linguistic variables for this input are defined as Negative (GX0), Zero (GX1), and Positive (GX2).

The outputs are the angular and linear velocities. Their acronyms are, respectively, VA and VL. The linguistic variables for the angular velocity output are defined as: Negative Big (VA0), Negative Small (VA1), Zero (VA2), Positive Small (VA3) and Positive Big (VA4). The linguistic variables for the linear velocity output are defined as Zero (VL0), Small (VL1), Medium (VL2), Big (VL3), and Very Big (VL4).

Figures 5, 6, 7 and 8 display the fuzzy controller surfaces. Figure 5 exhibits the angular velocity surface utilizing the alignment error and the orientation error. Figure 6 exhibits the linear velocity surface utilizing the alignment error and the orientation error. Figure 7 exhibits the linear velocity surface utilizing the orientation error and the weld bead type. Figure 8 exhibits the linear velocity surface utilizing the gravity and the weld bead type.

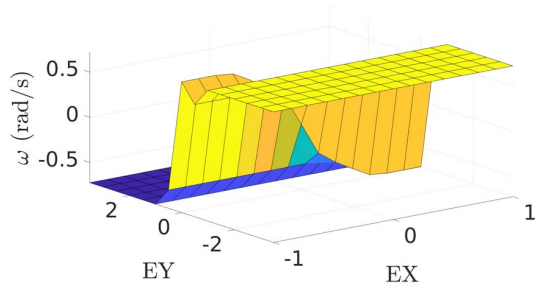

Fig. 5: Fuzzy controller surface for angular velocity output with the alignment error and the orientation error input

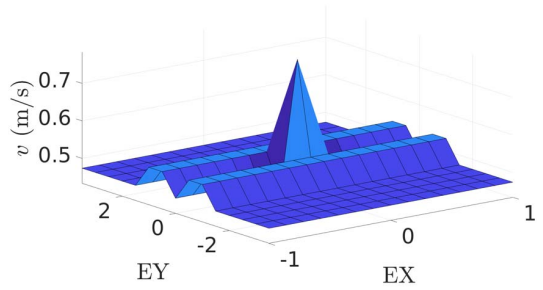

Fig. 6: Fuzzy controller surface for linear velocity output with the alignment error and the orientation error input

The rules for the controller are shown in Tables I, II, III and IV. Table I shows the rules for the angular velocity. The

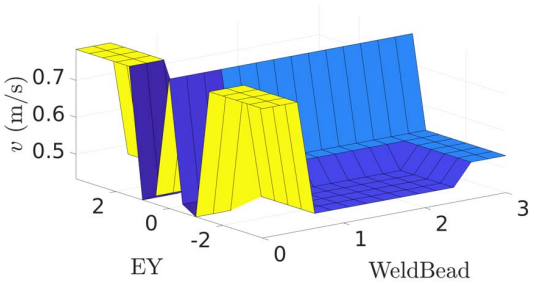

Fig. 7: Fuzzy controller surface for linear velocity output with the orientation error and the weld bead type input

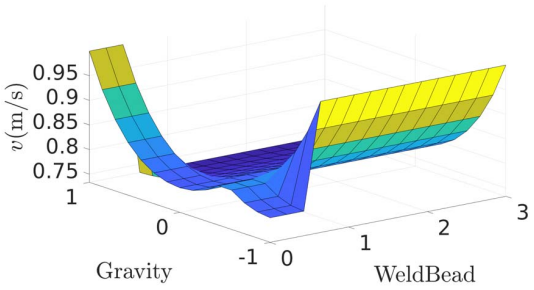

Fig. 8: Fuzzy controller surface for linear velocity output with the gravity and the weld bead type input

first column represents orientation error input value, and the first line represents the alignment error input value. The other three tables show the rules for the linear velocity. Table II considers the orientation error and the alignment error input values. Table III considers the orientation error and the weld bead type. Table IV considers the gravity and the weld bead type

TABLE I: Rule base for angular velocity.

EY \ EX	EX0	EX1	EX2	EX3	EX4
EY0	VA4	VA4	VA4	VA4	VA4
EY1	VA4	VA4	VA4	VA4	VA4
EY2	VA3	VA3	VA3	VA3	VA3
EY3	VA4	VA3	VA2	VA1	VA0
EY4	VA1	VA1	VA1	VA1	VA1
EY5	VA0	VA0	VA0	VA0	VA0
EY6	VA0	VA0	VA0	VA0	VA0

TABLE II: Rule base for linear velocity considering the alignment error and the orientation error

EY \ EX	EX0	EX1	EX2	EX3	EX4
EY3	VL0	VL1	VL3	VL1	VL0

VI. EXPERIMENTAL RESULTS

The experimental results of Sections III and IV were performed on a plate from a spherical storage tank. Its

TABLE III: Rule base for linear velocity considering the orientation error and the weld bead type

TS \ EY	EY0	EY1	EY2	EY4	EY5	EY6
TS0	VL3	VL1	VL0	VL0	VL1	VL3
TS12	VL0	VL2	VL2	VL2	VL2	VL0

TABLE IV: Rule base for linear velocity considering the gravity and the weld bead type

TS \ GX	GX0	GX1	GX2
TS0	VL2	VL2	VL3
TS12	VL3	VL2	VL1
TS3	VL3	VL2	VL1

dimensions are, approximately, 190 centimeters wide and 60 centimeters long. A weld bead is located in the center of the plate. Figure 9 shows an image of the described object.

Fig. 9: Plate used in the validation

The experimental results of Section V were simulated using V-REP (Virtual Robot Experimentation Platform). V-REP is a 3D robot simulator based on a distributed control architecture, and it allows the modeling of robotic systems similar to the reality [15]. Figure 10 presents an image of the scene in V-REP used for testing the concepts in this work. The tank is represented in grey, and the weld beads are represented in red.

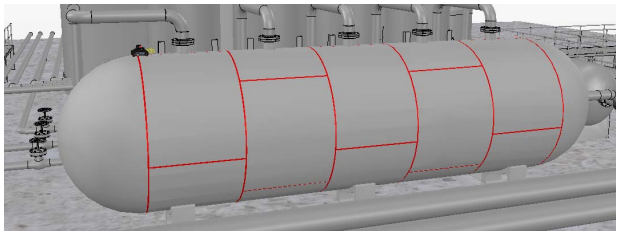

Fig. 10: Scene to validate the work

The data filtering, weld bead recognition, and control were implemented in python and ROS (Robot Operating System). ROS is a middleware, and its a collection of tools and libraries to simplify the programming in robotics [16]. The SciKit-Fuzzy [17] and SciPy [18] libraries were utilized in the implementation of the controller.

The validation of Section IV were made analyzing the sensor response and the result obtained by the algorithm proposed in this work. The measured data were visualized using the ROS visualizer, Rviz.

Figure 11a shows a picture of the data measured by the line profile sensor. Figure 11b presents the signal after the filtering with the low-pass FIR digital filter. Figure 11c displays the tank estimation calculated in the weld bead recognition. Figure 11d exhibits the linearized signal with the weld bead center estimation. The red dot is the estimation of the weld bead center. It is possible to observe that the algorithm is working correctly, once the dot is in the middle of the weld bead limits.

(a) Raw signal from the line profile sensor.

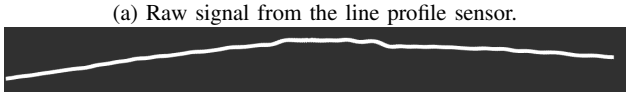

(b) Signal after the data filtering.

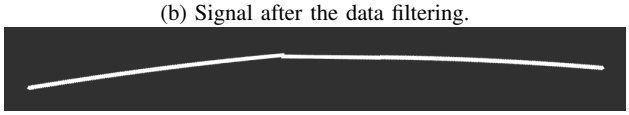

(c) Tank estimation.

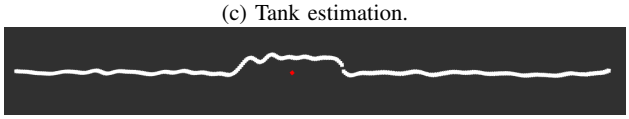

(d) Signal after the weld bead recognition.

Fig. 11: Rviz visualizations.

The validation of Section V was split into two experiments. In the first situation, the robot was required to follow a straight weld bead. In the second situation, the robot was required to turn at the weld bead joint.

Figure 12 displays the distance error module in the robot position in the first experiment. The controller's steady-state error and settling time were about 3 millimeters and 5 seconds, respectively. Figure 13 shows the angle error during the turn of the robot. The degrees in the graphic are caused by the difference among the publications over ROS. The controller's steady-state error and settling time were nearly 0.2 radians and 10 seconds, respectively.

It is possible to claim that the results obtained are acceptable, analyzing the information collected. The trajectory control is working. Then, the robot can track and navigate through the weld beads. However, the accuracy of the controller at turns was not at the expected level.

The main restriction of the robot is its maneuverability. When compared to other climbing robots, like [8], the AIR-1 lacks positioning precisely the robot. Its reason is the difference in degrees of freedom. Furthermore, The limitation of the robot for making small adjustments, caused by the magnetic wheels, leads to a steady-state error.

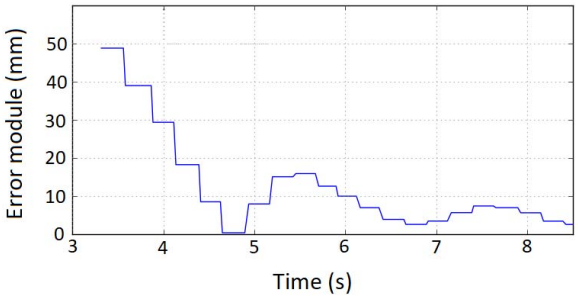

Fig. 12: Distance error

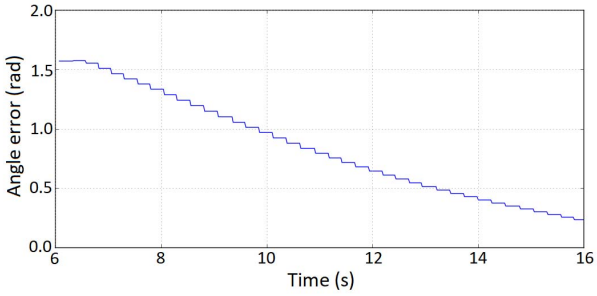

Fig. 13: Angle error

Although the satisfactory results, other variables have to be considered to achieve a more realistic system and improved the obtained results, for example, the slip of the robot.

Moreover, the absence of obstacles is a simplification applied in this work. Another proximity sensor, such as an ultrasonic sensor or a Light Detection And Ranging sensor, is needed to implement the obstacle deviation. This factor is an essential aspect of a real application, once the presence of obstacles is unavoidable.

VII. CONCLUSION

This paper presented an autonomous inspection robot, which can recognize and navigate the weld bead. The line profile sensor was used to measure the relative location of weld beads about the robot. An algorithm is designed to recognize the weld bead. A fuzzy controller controls the robot's velocity to track the weld bead.

The results show that the solution discussed in this article can track and follow a weld bead in a cylindrical tank. Nevertheless, the precision at turns needs to be improved. Furthermore, the AIR-1, in this approach, is not capable of realizing obstacle deviation.

Future works will consider other variables to improve the precision of the controller. Other perception sources could be added to allow the obstacle deviation to the robot. The realization of the controller tests in a real robot must be done.

REFERENCES

[1] L. Zhang, J. Jiao, Q. Ye, Z. Han, and W. Yang, "Robust weld line detection with cross structured light and hidden markov model," in *2012 IEEE International Conference on Mechatronics and Automation*. IEEE, 2012, pp. 1411–1416.

[2] T. Eiammanussakul, J. Taoprayoon, and V. Sangveraphunsiri, "Weld bead tracking control of a magnetic wheel wall climbing robot using a laser-vision system," in *Applied Mechanics and Materials*, vol. 619. Trans Tech Publ, 2014, pp. 219–223.

[3] K. J. Kim, H. W. Roh, H. K. Leem, R. S. Leem, G. Changwon, and S. J. Lee, "Application of a robot to grinding welding-beads remained in removal of working pieces for shipbuilding," *WMSCI08*, 2008.

[4] X. Lü, K. Zhang, and Y. Wu, "The seam position detection and tracking for the mobile welding robot," *The International Journal of Advanced Manufacturing Technology*, vol. 88, no. 5-8, pp. 2201–2210, 2017.

[5] O. Kermorgant, "A magnetic climbing robot to perform autonomous welding in the shipbuilding industry," *Robotics and Computer-Integrated Manufacturing*, vol. 53, pp. 178–186, 2018.

[6] Z. Gui, Y. Deng, Z. Sheng, T. Xiao, Y. Li, F. Zhang, N. Dong, and J. Wu, "Design and experimental verification of an intelligent wall-climbing welding robot system," *Industrial Robot: An International Journal*, vol. 41, no. 6, pp. 500–507, 2014.

[7] H. B. Santos, M. A. S. Teixeira, A. S. de Oliveira, L. V. R. Arruda, and F. Neves-Jr, "Scheduled Fuzzy Controllers for Omnidirectional Motion of an Autonomous Inspection Robot with Four Fully Steerable Magnetic Wheels," in *2016 XIII Latin American Robotics Symposium and IV Brazilian Robotics Symposium (LARS/SBR)*, Oct 2016, pp. 263–268.

[8] H. B. Santos, M. A. S. Teixeira, A. S. de Oliveira, L. V. R. de Arruda, and F. Neves-Jr., "Quasi-Omnidirectional Fuzzy Control of a Climbing Robot for Inspection Tasks," *Journal of Intelligent & Robotic Systems*, vol. 91, no. 2, pp. 333–347, Aug 2018.

[9] R. V. Espinoza, A. S. de Oliveira, L. V. R. de Arruda, and F. N. Junior, "Navigation's Stabilization System of a Magnetic Adherence-Based Climbing Robot," *Journal of Intelligent & Robotic Systems*, vol. 78, no. 1, pp. 65–81, Apr 2015.

[10] R. S. da Veiga, A. S. de Oliveira, L. V. R. de Arruda, and F. N. Junior, "Localization and navigation of a climbing robot inside a lpg spherical tank based on dual-lidar scanning of weld beads," in *Robot Operating System (ROS)*. Springer, 2016, pp. 161–184.

[11] M. A. S. Teixeira, H. B. Santos, N. Dalmedico, L. V. R. de Arruda, F. Neves-Jr., and A. S. de Oliveira, "Intelligent environment recognition and prediction for ndt inspection through autonomous climbing robot," *Journal of Intelligent & Robotic Systems*, vol. 92, no. 2, pp. 323–342, Oct 2018.

[12] L. Electronic. (2019) Lrs 36/6 - line profile sensor. [Online]. Available: https://www.leuze.com/en/deutschland/produkte/messende_sensoren/3d_sensoren_1/lichtschnittsensoren_1/lrs_7/selector.php?supplier_aid=50111330&grp_id=1331722677208&lang=eng

[13] D. G. Manolakis and V. K. Ingle, *Applied digital signal processing: theory and practice*. Cambridge University Press, 2011.

[14] R. L. Burden and D. J. Faires, *Análise númerica*. Cengage Learning, 2008.

[15] C. Robotics, "Coppelia robotics v-rep: Create. compose. simulate. any robot." 2019. [Online]. Available: http://www.coppeliarobotics.com/

[16] ROS, "Ros.org - powering the worlds robots," 2019. [Online]. Available: https://www.ros.org/

[17] J. Warner, J. Sexauer, Scikit-Fuzzy, Twmeggs, S. Alexandre M., Aishwarya Unnikrishnan, G. Castelo, F. Batista, T. G. Badger, and Himanshu Mishra, "Scikit-fuzzy 0.3.1," 2017. [Online]. Available: https://zenodo.org/record/1002946

[18] E. Jones, T. Oliphant, P. Peterson *et al.*, "SciPy: Open source scientific tools for Python," 2001. [Online]. Available: http://www.scipy.org/